UDK 532/533; 536; 538.9

K. HEINZINGER, G. PÁLINKÁS

ON THE SOLVATION OF IONS IN METHANOL

A flexible three-site model for methanol was recently employed in Molecular Dynamics simulations of 0,6 molal $MgCl_2$ and NaCl solutions. The ion-methanol and ion-ion potential functions were derived from ab initio calculations. The structural properties of the solutions are discussed on the basis of radial distribution functions, the orientation of the methanol molecules, and their geometrical arrangement in the solvation shells of the ions. Average potential energies and pair interaction energy distributions are reported. The dynamical properties of the solutions are calculated from various autocorrelation functions. Results are presented for the influence of the individual ions on self-diffusion coefficients, hindered translations, librations, and internal vibrations of the methanol molecules.

1. Introduction

The methanol molecule is the simplest organic compound that has both hydrophobic and hydrophilic groups and that forms strong hydrogen bonds via the latter groups with other solvent molecules or ions. Although methanol has such an interesting character as a solvent, the number of studies of structural and dynamical properties of methanolic solutions is still small [1].

The most extensive knowledge on the solvation of ions is based on computer simulations. Structural properties of the solvation shells of Na^+ and CH_3O^- were reported by Jorgensen and Chandrasekhar [2] from Monte-Carlo (MC) calculations where one ion was surrounded by 127 methanol molecules and of CL^- by Impey et al. [3]. Furthermore, an extended RISM analysis on ion association in an NaCl solution in methanol has been published by Hirata and Levy [4].

Significantly more detailed information has been deduced from Molecular Dynamics (MD) simulations of 0,6 molal NaCl [5] and $MgCl_2$ [6] solutions. Besides the structural also the dynamical properties of these solutions have been calculated. A flexible methanol model has been employed in these simulations which had proved its usefulness in the case of pure methanol [7]. Therefore, the effect of the ions on the intramolecular properties of methanol have been reported additionally.

The structure of the $MgCl_2$ solution has been compared with *X*-ray diffraction measurements [6]. Unfortunately neutron diffraction measurements with isotopic substitution-which proved to be a powerful tool in the determination of ion-water radial distribution functions (RDFs)-have not been reported so far for electrolyte solutions in methanol. Only pure methanol has been investigated in this way [8].

The self-diffusion coefficients of the ions and the methanol molecules in an NaCl solution have been measured by Hawlicka [9, 10] and can serve as a check on the quality of the pair potential employed in the simulation. Furthermore, from a series of IR studies of LiCl and $MgCl_2$ solutions in methanol at low temperatures Strauss and Symons [11] have evaluated the effect of Cl^- on the OH stretching frequency of the methanol molecules in its first solvation shell. The use of a flexible methanol model in the simulation and the division of all methanol molecules in the solution into three subsystems-bulk, solvation shell molecules of cation and anion-enables the calculation of the single ion effect on various properties of the methanol molecules, too.

In the next chapter the pair potentials employed in the simulations of the solutions are described and some details of the simulations are given. In chapter three structural, energetical, and dynamical properties of the solutions are reported and compared with experimental data. Differences in the solvation shells of the ions between methanolic and aqueous solutions are discussed.

ISSN 0452-9910. Cond. Mat. Phys. 1993. N 2.

2. Pair potentials

The potential describing the interaction between two methanol molecules is based on a flexible three-site model, consisting of an oxygen atom, a hydrogen atom, and the methyl group as a whole. The total potential consists of an intra- and an intermolecular part:

$$V(r_{\alpha\beta}, \rho_i) = V_{\text{intra}}(\rho_i) + V_{\text{inter}}(r_{\alpha\beta}), \tag{1}$$

where the ρ_i are the internal coordinates and the $r_{\alpha\beta}$ the distances between sites in different molecules.

The intramolecular potential has been chosen in the form proposed by Carney, Curtiss, and Langhoff (CCL) for water [12]:

$$V_{\text{intra}}(\rho_i) = \Sigma I_{ij}\rho_i\rho_j + \Sigma L_{ijk}\rho_i\rho_j\rho_k + \Sigma L_{ijkl}\rho_i\rho_j\rho_k\rho_l,$$

$$\text{with } \rho_1 = (r_{\text{OH}} - r^e_{\text{OH}})/r_{\text{OH}}, \quad \rho_2 = (r_{\text{CO}} - r^e_{\text{CO}})/r^e_{\text{CO}}$$

$$\text{and } \rho_3 = (\alpha_{\text{COH}} - \alpha^e_{\text{COH}})/\alpha^e_{\text{COH}}. \tag{2}$$

The quantities r^e_{OH}, r^e_{CO}, and α^e_{COH} are the gasphase equilibrium values being 0,9451 Å, 1,425 Å and 108,53°, respectively. The potential constants used in the simulations are given in Table 1. The strong reduction of the number of parameters is based on the approximation that the C—O stretching and the bending vibrations are harmonic, the interactions between the O—H and the C—O stretching vibration can be neglected, and only interactions between the O—H stretching and C—O—H bending vibrations which are linear in ρ_3 need to be taken into account [7].

Table 1. **Potential constants for the intramolecular potential energy of the methanol molecule (in kJ/mol) [7]. The notations are according to Eq. (1)**

ρ_1^2	2138,0	$\rho_1^2\rho_3$	450,3
ρ_2^2	2241,7	$\rho_1\rho_4$	5383,7
ρ_3^2	452,6	$\rho_1^3\rho_2$	661,3
ρ_1^3	—4522,5		

The potentials describing the intermolecular interactions can be separated in a Coulombic and non-Coulombic term:

$$V^{\text{inter}}_{\alpha\beta}(r_{\alpha\beta}) = q_\alpha q_\beta e^2/r_{\alpha\beta} + V'_{\alpha\beta}(r_{\alpha\beta}). \tag{3}$$

The charges assigned to the three sites are $q_{\text{O}} = -0{,}6\,|\,e\,|$, $q_{\text{H}} = 0{,}35\,|\,e\,|$ and $q_{\text{CH}_3} = 0{,}25\,|\,e\,|$. They yield a dipole moment of 1,93 D for the gas-phase geometry and lead to approximate agreement with the experimental dimerization energy.

The non-Coulombic parts of the O—O, O—H and H—H potentials are taken from the BJH model for water [13] and given by:

$$V'_{\text{OO}}(r) = 111889/r^{8,86} - 1{,}045\,\{\exp[-4(r-3{,}4)^2] - \exp[-1{,}5(r-4{,}5)^2]\}, \tag{4a}$$

$$V'_{\text{OH}}(r) = 26{,}07/r^{9,2} - 41{,}79/\{1 + \exp[40(r-1{,}05)]\} - 16{,}74/\{1 + \exp[5{,}493(r-2{,}2)]\}, \tag{4b}$$

$$V'_{\text{HH}}(r) = 418{,}33/\{1 + \exp[29{,}9(r-1{,}968)]\}. \tag{4c}$$

While the non-Coulombic term for the CH_3—H interaction is assumed to be zero, the ones for CH_3—CH_3 are described by a (12; 6) Lennard — Jones potential with parameters taken from Jorgensen (CH_3—CH_3: $\sigma = 3{,}86$ Å, $\epsilon = 0{,}7584$ kJ/mol; CH_3—O: $\sigma = 3{,}4$ Å, $\epsilon = 0{,}7449$ kJ/mol) [14].

The ion-methanol and ion-ion interaction energies were obtained from ab initio calculations. They were calculated for each complex for several hundred configurations and fitted to the analytical form:

$$V_{ij}(r) = Q_{ij}/r + A_{ij}/r^8_{ij} + B_{ij}\exp[-C_{ij}r]. \tag{5}$$

The parameters are listed in Table 2. Fig. 1 shows contours of the fitted potential surface for the Mg^{2+}-methanol and Cl^--methanol complexes with the ions

in the COH-plane as example. The minimum for the Mg^{2+}-complex was found to be —350 kJ/mol, about 50 kJ/mol lower than for the Mg^{2+}-water complex [15]. In the case of water the minimum is positioned directly in the anti-dipole direction, while it is found slightly off this direction for methanol. A linear hydrogen bond formation leads to the lowest energy minimum for both

Table 2. **Parameters for the ion-methanol pair potentials according to Eq. (5)**

i	j	Q_{ij} [kJAmol^{-1}]	A_{ij} [kJAmol^{-1}]	B_{ij} [kjmol^{-1}]	C_{ij} [Å^{-1}]	S_{ij}	Ref.
Mg	O	—1667,22	—721,86	$4{,}0778 \cdot 10^5$	4,3937	2	[6]
Mg	H	972,55	—7,2096	$4{,}2904 \cdot 10^1$	0,0275	2	[6]
Mg	C	694,68	—232,28	$1{,}8277 \cdot 10^4$	2,6485	2	[6]
Na	O	—833,61	—172,19	$2{,}5323 \cdot 10^5$	4,1501	2	[5]
Na	H	486,27	593,29	$-8{,}3273 \cdot 10^2$	0,9591	2	[5]
Na	C	347,34	—274,93	$5{,}1164 \cdot 10^4$	2,7930	2	[5]
Cl	O	833,61	127,00	$1{,}4529 \cdot 10^5$	3,1999	2	[6]
Cl	H	—486,27	—193,37	$2{,}5086 \cdot 10^4$	3,3082	2	[6]
Cl	C	—347,34	6,7657	$5{,}9250 \cdot 10^5$	3,2984	2	[6]
Mg	Mg	5556,5	—1479,6	$1{,}8223 \cdot 10^6$	6,3600	6	[15]
Mg	Cl	—2778,6	—2006,5	$1{,}1851 \cdot 10^5$	2,6500	2	[15]
Na	Na	1389,4	991,35	$1{,}0178 \cdot 10^6$	5,5909	6	[5]
Na	Cl	—1389,4	—78,985	$1{,}7168 \cdot 10^5$	3,1940	2	[5]
Cl	Cl	1389,4	—28672	$9{,}1704 \cdot 10^5$	3,3863	6	[5]

the Cl^--water and Cl^--methanol complexes. It is found to be —50 kJ/mol for methanol, which is about 10 % lower than for water. The ion-ion pair potentials employed here for the $MgCl_2$ solution are the basic cube contained 400 methanol molecules, 8 cations, and either 16 or 8 chloride ions. With the experimental densities a sidelength of 30,14 Å results for both solutions.

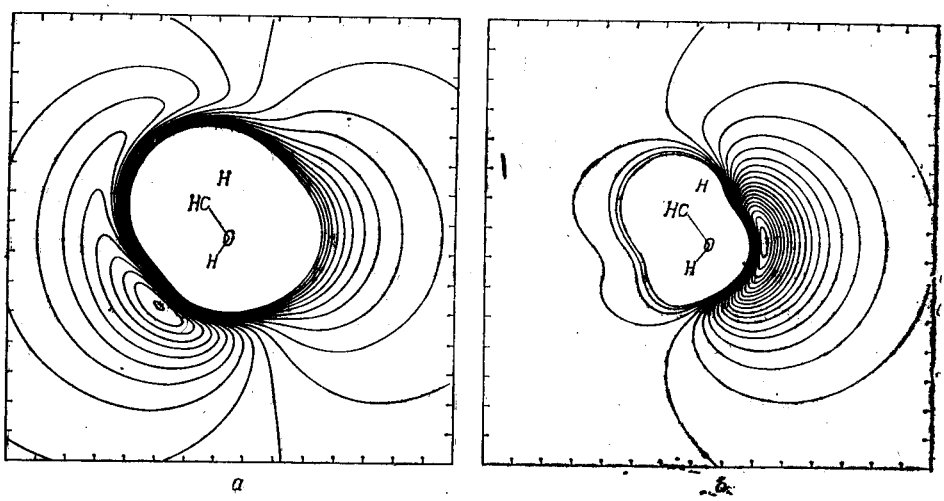

Fig. 1. The two basic conformations of THF

The Ewald summation was employed for all Coulombic interactions and the shifted force potential method with a cut-of length of 15,07 Å for the non-Coulombic parts of the potentials. The systems were equilibrated during several thousand time steps before the collection of data was started. With a time step of 0,25 fs the simulation extended over 5,5 ps for the $MgCl_2$ and 7 ps for the NaCl solution at average temperatures of 319 K and 292 K, respectively. During the simulations the velocities were not rescaled in order to get reliable velocity autocorrelation functions. The stability of the total energy was better than 0,5 %

3. Results and discussion

Radial Distribution Functions (RDF). In Fig. 2 the ion-oxygen, ion-hydrogen, and ion-carbon RDFs, $g_{\alpha\beta}(r)$, are drawn together with their corresponding running integration numbers. The Cl^- RDFs are depicted only from the simulation of the NaCl solution. They are not very different from those from the $MgCl_2$ solutions as can be seen from the characteristic values of the $g_{\alpha\beta}(r)$ and $n_{\alpha\beta}(r)$ listed in Table 3.

All Mg^{2+}-methanol RDFs show very sharp and well-separated first peaks. The Mg—O nearest neighbor distance is very similar to that found from a simulation of an aqueous $MgCl_2$ solution. The first peaks in $g_{MgO}(r)$ and $g_{MgH}(r)$ are narrower and about three times as high as in an aqueous solution [15]. These differences can be attributed, at least partly, to the stronger Mg^{2+}-methanol interaction when compared with that of Mg^{2+}-water, as mentioned above. The existence of a well defined first solvation shell is further established by the fact that Mg—O, Mg—H and Mg—C RDFs become zero at the end of the first peak and all three $n(r)$ result in almost exactly six nearest neighbors. Also the existence of a second solvation shell can be inferred from the RDFs. It is again more strongly pronounced than in the aqueous solution but comprises only about seven methanol molecules instead of 15 water molecules. This difference has to be attributed to the fact that only one possibility exists for hydrogen bonding between the methanol molecules in the first and second solvation shell.

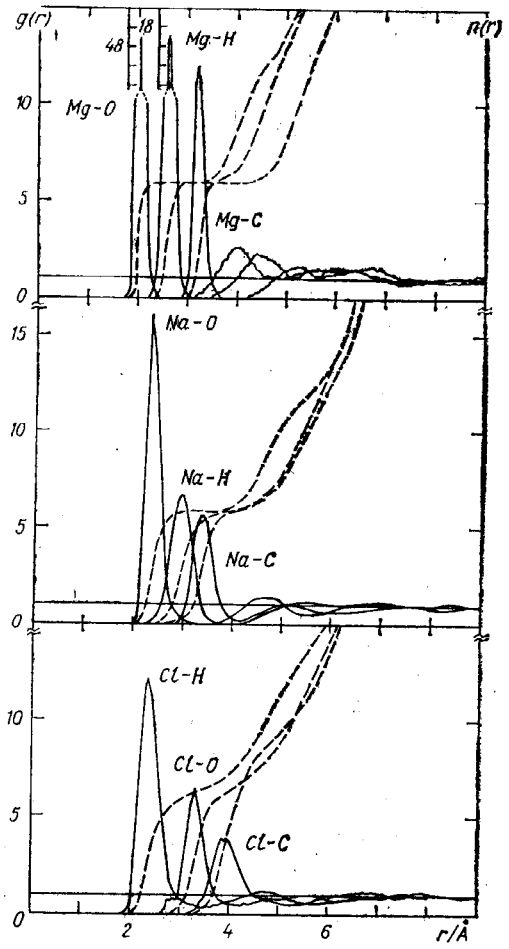

Fig. 2. Ion-oxygen, ion-hydrogen, and ion-carbon radial distribution functions and running integration numbers from MD simulations of 0,6 molal $MgCl_2$ and NaCl solutions in methanol. The Cl^- RDFs are taken from the simulation of the NaCl solution

The peaks in the Na^+-methanol RDFs are much less pronounced than the corresponding ones for Mg^{2+}, consistent with the larger size and smaller charge of Na^+. While the positions of the first peak in $g_{NaO}(r)$ and $g_{NaH}(r)$ are very similar to those in BJH water they are twice as high [16], a result which has to be attributed — at least partly — to the about 10 % lower potential minimum in the Na^+-methanol pair potential. The solvation number for Na^+ in methanol is found to be 5,8, which is exactly the same as in water. Robinson and Symons [17] deduced from IR overtone spectroscopy a solvation number of 5,7 for Na^+ in methanol. Because of this close agreement of the solvation numbers between simulation and experiment, the number of methanol, molecules in the second solvation shell, which is not accessible by experiments, may be estimated reliably from the simulation to be 6,2. The second hydration shell of Na^+ contains again about twice as many molecules [16], for the same reasons as discussed above in the case of Mg^{2+}. The solvation number of 5,8 results from the fact that in 80 % of all cases Na^+ is solvated by 6 and in 20 % by 5 methanol molecules. Compared to the position of the minimum

in the Na^+-methanol pair potential the first maximum of $g_{NaO}(r)$ is shifted by 0,2 Å to larger distances. In water the same shift is less than 0,1 Å, which means that the repulsive interactions between the bulky methyl groups prevent a tighter binding of the solvated molecules. The Na^+-solvent pair potentials both in water and in methanol have their minima for an anti-dipole orientation at a Na—O distance of 2,2 Å. There is a qualitatively good agreement between the result from the MD simulation of the 0,6 molal solution and the MC calculation of one Na^+ in 127 TIPS methanol molecules as far as can be judged from the numbers given in [2].

Table 3. **Characteristic values of the radial distribution functions. R_i, r_{M_i} and r_{m_i} give the distances in Å, where for the i-th time $g_{\alpha\beta}(r)$ comes to unity, has a maximum and a minimum, respectively. The uncertainty is at least ±0,02 Å. The values for Cl^- are taken from the NaCl solution**

α	β	R_1	r_{M_1}	$g_{\alpha\beta}(r_{M_1})$	R_2	$n_{\alpha\beta}(R_2)$	r_{m_1}	$n_{\alpha\beta}(r_{m_1})$
Mg	O	1,85	2,00	49,3	2,28	5,9	2,5—3,0	6,0
Mg	H	2,35	2,61	17,7	2,88	5,9	3,0—3,4	6,0
Mg	C	3,00	3,21	12,0	3,48	5,8	3,8—4,2	6,0
Na	O	2,12	2,38	15,9	2,78	5,6	3,4	5,8
Na	O[a]	2,10	2,30	8,0	2,66	(5,5)	3,10	5,8
Na	H	2,57	2,95	6,9	3,38	5,6	3,8	5,9
Na	C	3,06	3,35	5,5	3,78	5,6	4,1	6,0
Cl	O	3,02	3,28	7,0	3,80	6,5	4,3	7,2
Cl	O[a]	2,95	3,18	3,4	3,60	(6,5)	3,87	7,7
Cl	O[b]	2,95	3,28	6,5	3,72	5,9	4,2	6,6
Cl	H	2,03	2,35	12,7	2,97	6,5	3,4	7,0
Cl	C	3,53	3,88	3,9	4,48	7,4	5,0	8,6

[a] From a 2,2 molal aqueous NaCl solution [16].
[b] From the 0,6 molal $MgCl_2$ solution in methanol.

In analogy to the cations, the first solvation shell of Cl^- is more pronounced in methanol than in water. The first peak in $g_{ClO}(r)$ is again twice as high as in water (Table 3). The separation between solvation shell and bulk molecules is sharper in methanol than in water, as can be seen from the value of $g_{ClO}(r)$ at r_{m1}, which is with 0,3 less than half of the corresponding value in water. The solvation number of Cl^- is found to be 7,2, which is similar to the hydration number of 7,7 in BJH water. The distribution of solvation numbers for Cl^- is much broader than for the cations (17,50, and 33 % for solvation numbers of 6,7, and 8, respectively). In the methanolic $MgCl_2$ solution the solvation number of Cl^- is only 6,6. This lower value results from the contact ion pair formation in the methanolic $MgCl_2$ solution, where a Mg^{2+} occupies the place of solvent molecules and thus reduces the solvation number of the anion (see below). This effect on the coordination and solvation numbers is well known from simulations of concentrated electrolyte solutions [18].

The Cl—H, Cl—O, and Cl—C RDFs can be compared with the results of an extended RISM analysis of an NaCl solution in methanol [4]. The positions of the first peaks in $g_{C.O}(r)$ and $g_{ClC}(r)$ resulting from the simulation appear at shorter distances and the peak heights are in all three cases higher than from the RISM analysis. It is not to be expected that these discrepancies have to be attributed to the simulations as the comparison of the Na—H and Na—C RDFs with the MC calculations by Jorgensen and Chandrasekhar show similar differences [2].

Ion-ion RDFs have also been calculated from both simulations, though because of the small number of ions in the sample and the time scale of 5,5 ps they are of lower statistical reliability. The RDFs for the like ions do not show any characteristic features and are, therefore not drawn here. The Mg—Cl RDF is shown in Fig. 3. The first sharp peak indicates contact ion pair forma-

tion. It can be seen from $n_{MgCl}(r)$ at about 4 Å that one out of four Mg^{2+} forms a contact ion pair. Obviously such an arrangement is rather stable, but one might expect that at significantly longer simulation times it will disappear. The second peak, below 6 Å, points to the existence of solvent shared ion pairs. The probability for their formation seems to be about the same as for contact ion pairs. The Na—Cl RDF gives no indication for contact ion pair formation. For a detailed comparison of the results from the MD simulation with those from an *X*-ray measurement of an $MgCl_2$ solution at the same concentration the reader is refered to Ref. [6].

Orientation of the Methanol Molecules. The orientation of the methanol molecules in the first solvation shells of Mg^{2+}, Na^+, and Cl^- are described by the distributions of cos Φ and cos Ψ, respectively. They are shown in Fig. 4 where also Φ and Ψ are defined in the insertions. The distributions demonstrate a strong preference for a trigonal orientation of the methanol molecules surrounding Mg^{2+} and Na^+ and for a linear hydrogen bond formation of the first solvation shell molecules with Cl^-. The preferential orientations are the same as in aqueous $MgCl_2$ and NaCl solutions [15, 16], but they are more pronounced here in accordance with the higher and narrower first peaks in the ion-oxygen and ion-hydrogen RDFs, as discussed above. The orientational efect of Mg^{2+} is significantly stronger than that of Na^+ indicated by the narrower distribution of cos Φ. There is no pronounced effect of the cations on the distribution of cos Ψ.

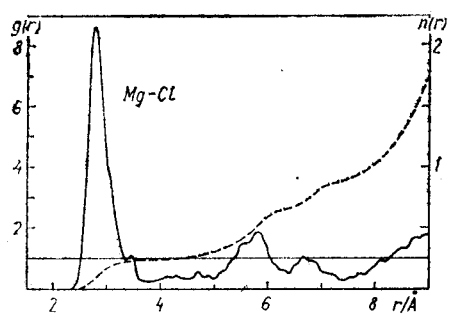

Fig. 3. Mg^{2+} — Cl^- radial distribution function and running integration number from an MD simulation of a 0,6 molal $MgCl_2$ solution in methanol [6]

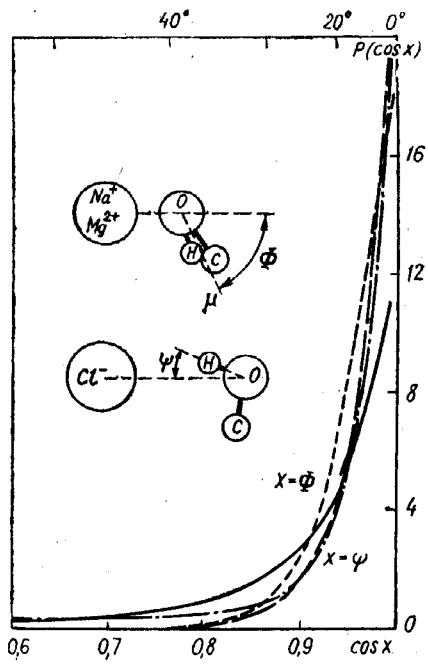

Fig. 4. Distribution of cos Φ and cos Ψ for the methanol molecules in the hirst solvation shells of Mg^{2+} (- - -), Na^+ (—) and Cl^- (— — — — NaCl; ..... $MgCl_2$), respectively, calculated from MD simulations of 0,6 molal $MgCl_2$ and NaCl solutions in methanol. μ is the dipole moment vector of the methanol molecule

In Fig. 5 the average values of cos (180 — Φ) and cos Ψ are presented as functions of the ion-oxygen distances. The almost monotonous decrease of the preferential orientation of the methanol molecules as a function of distance from Na^+ is interrupted only in the region between 3—4 Å. Reliable conclusions cannot be drawn from this deviation as there are only a small number of methanol molecules involved (see $g_{NaO}(r)$ in Fig. 2) and consequently the statistical significance is very limited. The situation is different for Mg^{2+} where a high degree of orientation is sustained without interruption from the first to the second solvation shell and where beyond 4,5 Å the preferential orientation slowly decreases in a similar way as for Na^+ but in general with slightly larger absolut values of cos (180 — Φ). In Fig. 5 the results from an MD simulation of a 2,2 molal aqueous NaCl solution are shown additionally for comparison [16]. The general features are very similar but the absolute

values of cos (180 — Φ) are much smaller demonstrating that the orientational order around an Na^+ in water does not reach as far as in methanol and is significantly less pronounced.

The average value of cos Ψ (*r*)-shown in the upper part of Fig. 5 — is almost one over the range of the first peak in g_{ClO} (*r*), in agreement with the strong preference for a linear hydrogen bond formation between Cl^- and the methanol molecules in its first solvation shell. It remains high (0,7—0,8) up to about 6 Å in the NaCl solution and decreases rapidly beyond this distance. This is again a significantly farther ranging orientational order than in the aqueous case [16]. The comparison with the methanolic $MgCl_2$ solution

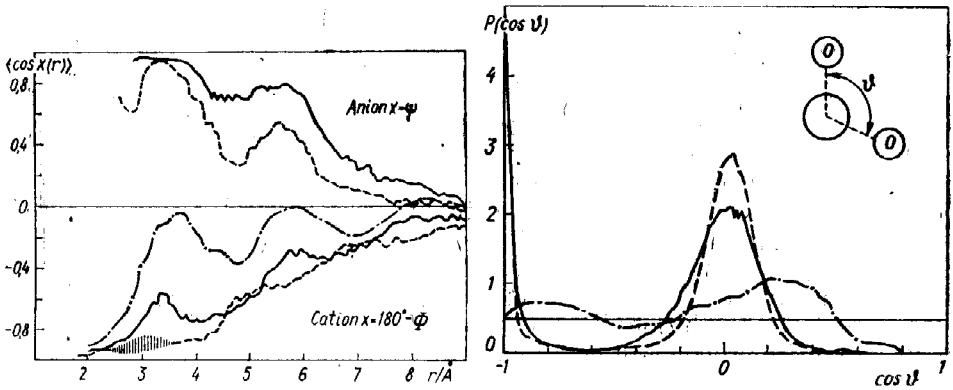

Fig. 5. Average values of cos Φ and cos (180 — Ψ) as functions of ion-oxygen distances, calculated from MD simulations of 0,6 molal $MgCl_2$ (dashed) and NaCl (full) solutions in methanol. Φ and Ψ are defined in the insertion of Fig. 4. The dotted line has been calculated from a simulation of a 2,2 molal aqueous NaCl solution [16]

Fig. 6. Distribution of cos ϑ where ϑ is defined as the oxygen-ion-oxygen angle calculated for the methanol molecules in the first solvation shells of Mg^{2+} (dashed), Na^+ (full) and Cl^- (dotted) from MD simulations of 0,6 molal $MgCl_2$ and NaCl solutions in methanol

shows that the solvation shell of Cl^- is much less disturbed in the NaCl solution at the same concentration. The methanol molecules at shorter distances, corresponding to the shoulder in g_{ClO} (*r*) below 3 Å, show an energetically less favourable orientation. They might belong at the same time to the first solvation shell of Mg^{2+} and Cl^- (solvent shared or contact ion pairs as discussed above) and where Mg^{2+} dominates the orientation. The second peak in ⟨cos Ψ (*r*)⟩ has no equivalent in g_{ClO} (*r*). The preferential orientation of the methanol molecules in the $MgCl_2$ solution relative to both ions extends significantly further than the one of the water molecules in an aqueous solution of equivalent concentration [15].

Solvation Shell Symmetries. The geometrical arrangement of the methanol molecules in the solvation shells of Mg^{2+}, Na^+ and Cl^- has been investigated by calculating the distribution of cos ϑ, shown in Fig. 6, where ϑ is defined in the insertion. The solvation shell of the cations is octahedrally structured as demonstrated by the maxima at 90° and 180°. As the volume of the first solvation shell-defined by r_{m1} — is smaller for Mg^{2+} than for Na^+ but has to accomodate the same number of methanol molecules, the sterical hinderance of the methyl groups prohibits larger deviations from the octrahedral geometry and more pronounced maxima. For the first solvation shell of Cl^- with its 7,2 methanol molecules no symmetry is found. *P* (cos ϑ) shows a practically uniform distribution over the whole range except for the excluded volume effect for cos $\vartheta > 0{,}8$, which results from the finite size of the methanol molecules.

Interaction Energies. The average energy of two methanol molecules as a function of their O—O distance, $\langle V_{MM}(r)\rangle$, and of a methanol molecule in the field of a Mg^{2+}, Na^+, and Cl^- as a function of the ion-O distance, $\langle V_{IonM}(r)\rangle$, are presented in Figs. 7 and 8, respectively. The integrated

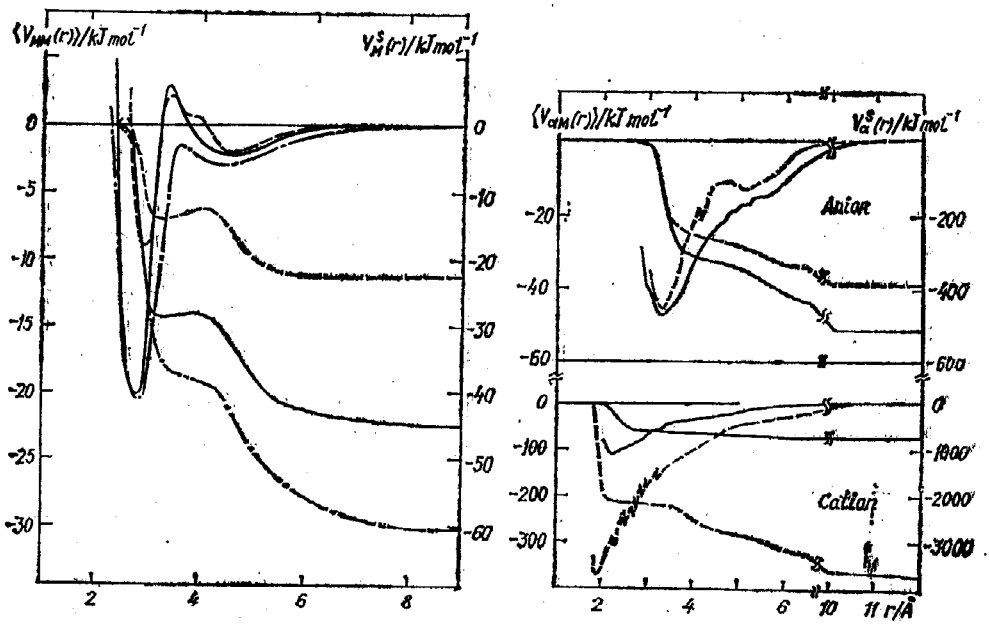

Fig. 7. Average potential energies of two methanol molecules as functions of their O—O distanee (left) and of a methanol molecules in the field of an ion (right) together with the running integrated interaction energies according to (4) calculated from simulations of 0,6 molal $MgCl_2$ (dashed) and NaCl (full) solutions and in pure methanol (dotted)

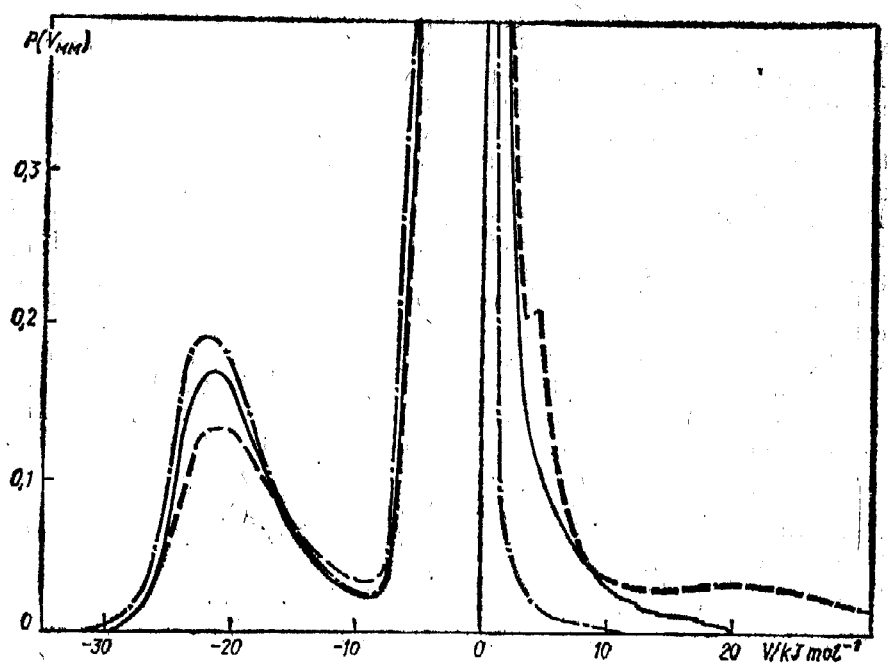

Fig. 8. Normalized pair interaction energy distributions for methanol-methanol from simulations of 0,6 molal $MgCl_2$ (dashed) and NaCl (full) solutions and pure methanol (dotted)

interaction energies, as defined by:

$$V_{\alpha}^{s}(r) = 4\pi\rho_{M} \int_{0}^{r} g_{\alpha O}(r)\ \langle V_{\alpha M}(r)\rangle\, r^{2} dr, \qquad (6)$$

are drawn additionally. ρ_M is the number density of the methanol molecules and α denotes either a methanol molecule or one of the ions.

In order to investigate the influence of the ions on the interaction energies between two methanol molecules, $\langle V_{MM}(r)\rangle$ and $V_{M}^{S}(r)$ for the 0,6 molal $MgCl_2$ and NaCl solutions are compared in Fig. 7 with those of pure methanol [7]. The comparison demonstrates that the ions strongly disturb the hydrogen bond formation of methanol. Obviously the 0,6 molal NaCl disturbs the methanol structure much less than the $MgCl_2$ solution at the same concentration.

Table 4. **Average values of bond lengths, bond angles, and dipole moments for the methanol molecules in the bulk and in the first solvation shells of the ions**

	R_{OH}/Å	R_{CO}/Å	R_{CH}/Å	α_{COH}	μ/D
bulk	0,966	1,427	1,939	106,7	1,99
Mg^{2+}	0,981	1,434	1,918	103,6	2,09
Na^{+}	0,966	1,427	1,940	106,8	1,99
Cl^{-}	0,965	1,426	1,937	106,7	1,99

The reduction of the minimum in $\langle V_{MM}(r)\rangle$ by a factor of more than two in the $MgCl_2$ solution results mainly from the interactions between the methanol molecules in the first solvation shell of Mg^{2+}. They are forced into energetically unfavorable orientations relative to each other by the strong influence of the Mg^{2+}. Their O—O distances in the octahedral symmetry are 2,83 Å, which is about the same distance as for the methanol dimer. The positive interaction energies in the distance as for the methanol dimer. The positive interaction energies in the distance range 3,3—4,0 Å which are very similar in both solutions seem to result from the combined effect of both ions on the relative orientation of two methanol molecules as it can occur near ion pairs and solvent shared ion pairs. A second minimum in $\langle V_{MM}(r)\rangle$ exists around 4,6 Å which almost coincides with the second peak in $g_{OO}(r)$ and indicates an energetically favorable orientation of two methanol molecules in this distance range. The relatively small disturbance of the solvent structure by Na^{+} and Cl^{-} leads to a reduction of the integrated interaction energy by only 25 %, which is much less than for the $MgCl_2$ solution where the reduction amounts to about 60 %.

The average potential energies of the methanol molecules in the field of the ions and their integrated interaction energies are also depicted in Fig. 7. The positions of the minima in the $\langle V_{\alpha M}(r)\rangle$ coincide for Na^{+} and Cl^{-} with those of the first peaks in the corresponding RDFs. It indicates that there is no steric hindrance between the methanol molecules in the first solvation shells of these two ions which could prevent them from occupying the energetically most favorable distances. In the Mg^{2+} case it is positioned slightly below that point. For Cl^{-} the minimum is about 10 % less deep than the pair potential minimum as a consequence of thermal motions and the interactions with other neighboring methanol molecules. For Na^{+} the depth is about the same. Unlike Cl^{-} the minimum in $\langle V_{MgM}(r)\rangle$ is deeper than the pair potential minimum. In spite of the same effects being active as in the chloride case they are overcompensated by the strong effect of the Mg^{2+} on the intramolecular geometry of the methanol molecules (Table 4 and discussion below), which results in an increase of the dipole moment and consequently a more negative pair interaction energy relative to the ab initio calculations where the gas phase geometry was employed.

The curves for $V_{\alpha}^{s}(r)$ show that for Mg^{2+} the first solvation shell is ener-

getically well defined and a second one is indicated, while for Na^+ and Cl^- even the first shell is not very pronounced. The far ranging preferential orientation of the methanol molecules relative to the cations, as demonstrated in Fig. 5, is also reflected in $\langle V_{\alpha M}(r)\rangle$ which even at 9 Å is different from zero. Consequently $V_\alpha^s(r)$ has not reached its limiting value at that distance. The first solvation shell contributes more than half of the total integrated interaction energies for all ions.

The pair interaction energy distribution for methanol — methanol interactions in the 0,6 molal $MgCl_2$ and NaCl solutions are compared in Fig. 8 with that for pure methanol [7]. At the negative energy side both distributions are very similar, indicating that the hydrogen bond structure of methanol is disturbed only slightly in the solution. The enhancement of the probability density in the range of positive interaction energies in both solutions is a consequence of the energetically unfavorable relative orientation of two methanol molecules in the solvation shells of the ions.

The ion-methanol pair interaction energy distributions, $P(V_{\text{ion}M})$, are depicted in Fig. 9. The positions of the peaks at the negative energy side practically coincide with the depth of the minima in $\langle V_{\alpha M}(r)\rangle$. The narrowness of the distributions is in accordance with the relatively narrow distributions of the orientations of the methanol molecules in the first solvation shells of the ions as shown in Fig. 4. The weak second solvation shell of Na^+, which can be seen from $g_{NaO}(r)$ in Fig. 3, appears also from an energetical point of view as a shoulder at about —30 kJ/mol. In the case of Mg^{2+} the second solvation shell leads even to a separate peak. For Cl^- the position of the maximum at negative energies appears slightly below—50 kJ/mol for both solutions in accordance with Fig. 7. There is a strong increase at the positive energy side with a shoulder at about 25 kJ/mol in the case of the $MgCl_2$ solution. These positive energies seem to result from methanol molecules which belong at the same time to the solvation shell of Mg^{2+} and Cl^- and where the strong effect of Mg^{2+} forces the molecules into an energetically unfavorable orientation relative to Cl^-.

The self-diffusion coefficients have been derived from the velocity autocorrelation functions with the help of the Green — Kubo relation:

$$D = \lim_{t\to\infty} \frac{1}{3} \int_0^t \langle v(0) * v(t')\rangle \, dt', \tag{7}$$

where the averages are calculated according to:

$$\langle v(0) * v(t)\rangle = \frac{1}{N_T N} \sum_{i=1}^{N_T} \sum_{j=1}^{N} v_j(t_i) * v_j(t_i + t), \tag{8}$$

and where N denotes the number of particles, N_T the number of time averages, and $v_j(t)$ the velocity of particle j at time t.

The normalized velocity autocorrelation functions for the ions and for the center of mass of all methanol molecules in the 0,6 molal $MgCl_2$ and NaCl solutions are shown in Fig. 10. In addition, they have been calculated separately for three methanol subsystems in the solutions, namely bulk methanol and the methanol molecules in the first solvation shells of the cations and the anions, in order to study in single ion effect on the translational motions of methanol. They are depicted also in Fig. 10. the first solvation shells are assumed to extend to the first minima in the corresponding ion-oxygen RDFs.

For a better comparison of their different time dependences the acf's are drawn only up to 1,2 ps while a correlation time of 2,5 ps is used in all cases for the evaluation of the self-diffusion coefficients. Their statistical error is estimated to be $\pm 0{,}2 \cdot 10^{-5}$ см²/s. It should be mentioned that because of the small Stokesradius of the 3-site PHH methanol model the calculated self-diffusion coefficients for methanol are expected to be about 30 % larger than the experimental ones [7] in accordance with the self-diffusion coefficient calculated from the simulation of the six-six PHH methanol model [19]. The

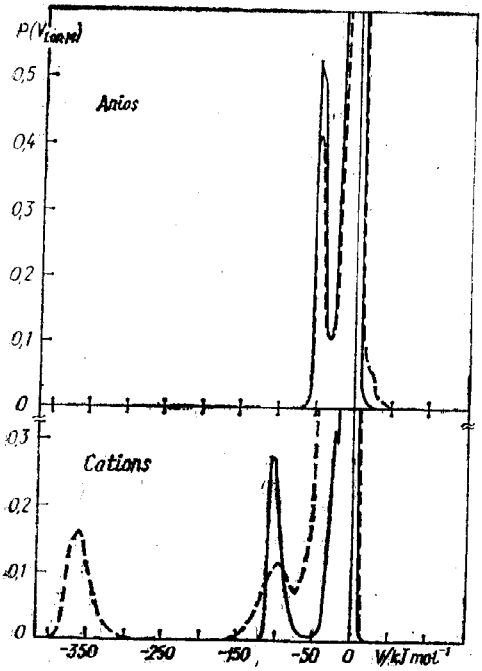

Fig. 9. Normalized ion-methanol pair interaction energy distributions from simulations of 0,6 molal $MgCl_2$ (dashed) and NaCl (full) solutions

various self-diffusion coefficients in the $MgCl_2$ solution are found to be 2,2, 0,6, and $2,0 \cdot 10^{-5}$ см²/s for methanol, Mg^{2+}, and Cl^-, respectively. For the three methanol subsystems they have been calculated to be 2,4, 0,5, and $2,0 \times 10^{-5}$ cm²/s for bulk methanol, solvation shell of Mg^{2+} and Cl^-, respectively. Exerimental self-diffusion coefficients for Mg^{2+} in methanol could not be found in the literature. The very low value for Mg^{2+}, which is similar to the one for Sr^{2+} and Li^+ in water [20, 21], is a consequence of its strong interactions with the solvent molecules in the first solvation shells as can be seen from the spectral densities of the hindered trans-

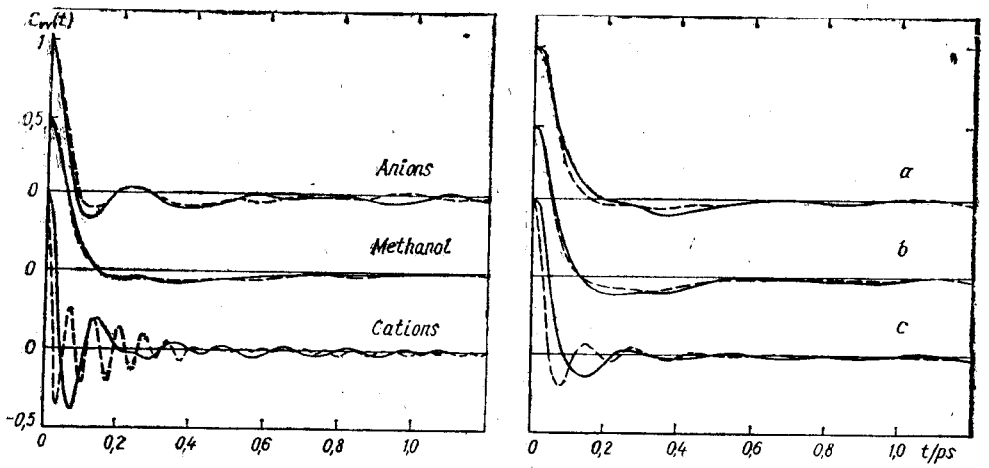

Fig. 10. Normalized velocity autocorrelation functions $\langle v(0) \cdot v(t)\rangle / \langle v(0)^2\rangle$ for the methanol molecules (center of mass), the cations, and the anions (left) and separately for bulk methanol (*a*) and the methanol molecules in the first solvation shells of Cl^- (*b*) and the cations (*c*) (right) calculated from MD simulations of 0,6 molal $MgCl_2$ (dashed) and NaCl (full) solutions

lational motions of Mg^{2+} discussed in the next section. This is, furthermore, confirmed by the self-diffusion coefficient of the methanol molecules in the first solvation shell of Mg^{2+}, which is in the limits of uncertainty the same as for the ion itself. The self-diffusion coefficients of Cl^- and of the methanol molecules in its first solvation shell are found to be nearly the same and only about 20 % lower than that of bulk methanol. The value for Cl^- calculated from simulations of various aqueous electrolyte solutions in only about half of that found here [20].

For a better comparison of the data for the NaCl solution with experimental ones all self-diffusion coefficients have been extrapolated to 298 K with the help of the experimentally determined temperature dependences [22]. The self-diffusion coefficient for the sodium ion, $D_{Na^+} = 1,2 \cdot 10^{-5}$ cm²/s, is in very good agreement with the measured value for an infinitely dilute

NaCl solution in methanol of $1{,}22 \cdot 10^{-5}$ cm²/s [9]. The self-diffusion coefficient of the methanol molecules in the first solvation shell of Na^+ is about 50 % larger than that of the ion itself. This shows the much weaker Na^+-methanol interaction than the Mg^{2+}-methanol one. The remaining influence of the Na^+ on the mobility of its solvation shell molecules remains significant when the self-diffusion coefficient is compared with that of bulk methanol, which has been calculated to be $2{,}7 \cdot 10^{-5}$ cm²/s. While the self-diffusion coefficients of the three methanol subsystems are not accessible experimentally, the value for all solvent molecules in the 0,6 molal NaCl which is with $2{,}6 \times \times 10^{-5}$ cm²/s slightly lower than that for bulk methanol compares favorably with the experimental one $2{,}23 \times \times 10^{-5}$ cm²/s for a 0,16 molal NaCl solution [10]. The value of $D_{Cl^-} = 0{,}9 \cdot 10^{-5}$ cm²/s from the simulation of the 0,6 molal NaCl solution can be compared with a measured one of $1{,}1 \cdot 10^{-5}$ cm²/s for a 0,013 molal solution [9]. There is a further decrease with increasing NaCl concentration

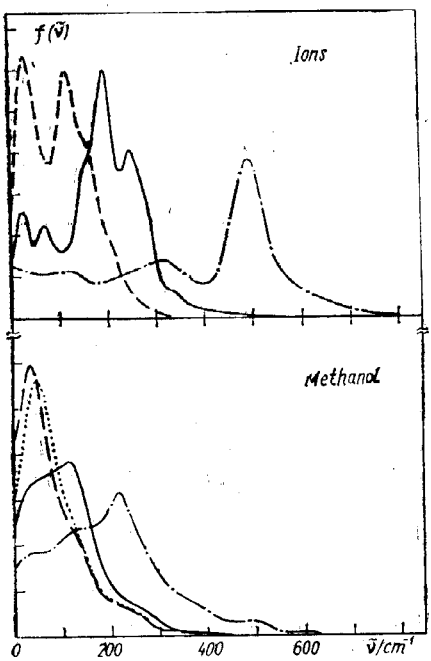

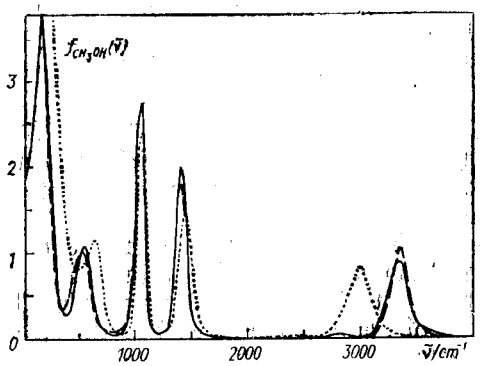

Fig. 11. Spectral densities of the hindered translations of the ions and of the methanol molecules (in arbitrary units) calculated from MD simulations of 0,6 molal $MgCl_2$ and NaCl solutions separately for bulk methanol (———), and the methanol molecules in the first solvation shells of Cl^- (from the NaCl solution) (- - - -), Mg^{2+} (— — —) and Na^+ (—)

Fig. 12. Total spectral densities of methanol(in arbitrary units) calculated separately for the molecules in the bulk (full) and in the first solvation shells of Cl^- (— — —) and Mg^{2+} (.....) from an MD simulation of a 0,6 molal $MgCl_2$ solution

expected from the experiments but an extrapoltion to significantly higher concentrations seems not to be warranted because of a lack of data. The self-diffusion coefficient for the methanol molecules in the first solvation shell of Cl^- is found to be $1{,}6 \cdot 10^{-5}$ cm²/s. Similar to the effect of Na^+ on its solvation shell molecules this value is significantly larger than that of the ion itself but much smaller than the one for bulk methanol.

Hindered Translations. The spectral densities of the hindered translational motions have been calculated by Fourier transformation:

$$f(\omega) = \int_0^\infty \frac{\langle v(0) * v(t) \rangle}{\langle v(0)^2 \rangle} \cos(\omega t)\, dt \qquad (9)$$

from the normalized velocity autocorrelation functions as shown in Fig. 10 and are presented in Fig. 11 for the ions and separately for the three methanol subsystems.

The Cl^- spectrum (shown here only for the NaCl solution as it is quite similar to that for the $MgCl_2$ solution) has a double peak with maxima at 35 and 125 cm^{-1}. In accordance with the assignment in the case of aqueous solu-

tions [23] the low frequency peak can be attributed to the motion of the bare anion while interactions of Cl^- with its neighbourhood lead to the peak at the higher wavenumber. Different from the aqueous case, where the second peak is reduced to a shoulder, the same height of both peak demonstrates again that the interactions of Cl^- with methanol are significantly stronger than with water. The main peak in the spectrum of the hindered translations of Na^+ appears at 200 cm^{-1} with a small satellite peak at 260 cm^{-1}. Because of the stronger Na^+-methanol compared with the Cl^--methanol interactions none of these frequencies can be assigned to the motion of the bare Na^+. The Mg^{2+} spectrum shows a single peak at about 500 cm^{-1} (Fig. 11). This high frequency for the hindered translation is expected from the velocity autocorrelation function (Fig. 10) and results from the motions of Mg^{2+} in the cage of the firmly attached six methanol molecules in its first solvation shell. This assignment explains also the small self-diffusion coefficient as it means that

Table 5. **Frequencies, in cm^{-1}, of the peak maxima in the total spectral densities of methanol calculated separately for the molecules in the bulk and in the first solvation shells of Mg^{2+}, Na^+ and Cl^-. The statistical uncertainty of the peak positions is estimated to be ± 10 cm^{-1}**

	bulk methanol	first solvation shell of		
		Cl^-	Na^+	Mg^{2+}
libration	534	522	540	628
CO stretch	1045	1045	1043	1064
COH bend	1406	1404	1407	1440
OH stretch	3344	3368	3291	2997

the ion can move only together with its six solvation shell molecules and this complex is further hindered by hydrogen bond formation between first and second solvation shell.

The maxima in the spectral densities of the hindered translations of the methanol molecules in the bulk and in the solvation shells of Cl^- and Na^+ appear at 35, 50 and 130 cm^{-1}, respectively. The small difference in the position of the maxima as well as the strong similarity in the whole range of the spectral densities for bulk methanol and the methanol molecules in the first solvation shell of Cl^- (Fig. 11) are in accordance with the conclusion drawn above from most of the properties discussed that the Cl^- has only a small influence on the properties of its surrounding methanol molecules. The Na^+ causes not only an almost 100 cm^{-1} blueshift of the maximum but results also in a very broad distribution in the spectral densities which is similar in shape to the one for the solvation shell molecules of Mg^{2+} except that in the Mg^{2+} case the maximum is shifted by about 200 cm^{-1} relative to bulk methanol.

Librations and Intramolecular Vibrations. It has been demonstrated in a preceding paper [7] that the methanol model employed in these simulations describes correctly the gas-liquid frequency shift of the intramolecular vibrations. The change of the intramolecular O—H distance on condensation corresponds to this shift according to the empirical proportionality factor between the O—H stretching frequency and the O--H distance of 20 000 $cm^{-1}/Å$ [24]. As the model describes correctly the intramolecular changes upon hydrogen bond formation it is expected that the effect of the ions on the intramolecular properties of methanol can also be calculated reliably from these simulations.

In order to calculate the single ion effect on the intramolecular geometry and the vibrations, the 400 methanol molecules in the solution are divided again into the three subsystems described above. The average values of the bond lengths and the bond angles are given in Table 4. The total spectral densities of the vibrational motions have been calculated separately for the three subsystems as the weighted sum of the Fourier transforms of the normalized velocity autocorrelation functions of the three sites in the methanol molecule. The results for the $MgCl_2$ solution are shown in Fig. 12 and the positions of the peak maxima are listed in Table 5.

In the limits of statistical uncertainty the spectral of the librations as well as those of the CO stretching and COH bending vibrations are not affected by Na^+ and Cl^-, as can be seen from Table 5. But the Na^+ shifts the OH stretching frequency of its solvation shell molecules to the red by about 50 cm^{-1} relative to pure methanol. In the case of Cl^- a blueshift of about 25 cm^{-1} has been calculated from the simulation. This small difference would hardly be considered significant if there would not be strong indications for such a blueshift caused by Cl^- from IR measurements of LiCl and $MgCl_2$ solutions at a temperature of —125 °C by Strauss and Symons [11]. The difference between the experimental blueshift of 100 cm^{-1} and the 24 cm^{-1} calculated from the simulation may have to be attributed, at least partly, to the low temperature at which the experiments were performed. Further indications for such an effect result from Raman measurements of LiCl solutions in ethanol by Yamauchi and Kanno [25] at liquid nitrogen temperatures who attributed a blueshift of similar size (100 cm^{-1}) to the Cl^--ethanol interactions.

The Mg^2 causes a blueshift of the librational, the C—O stretching and the COH bending frequencies and a strong redshift of the O—H stretching frequency of the methanol molecules of its first solvation shell relative to bulk methanol (Fig. 12 and Table 5). The blueshift of the librational frequencies and the bending vibration seems to be significant while the one of the C—O stretching vibration is hardly outside the limits of statistical uncertainly. There is no information from experiments on ion induced frequency shifts in the range below 2000 cm^{-1}.

The redshift of the O—H stretching frequency of methanol caused by Mg^{2+} is of similar size as the shifts which result from the interactions of Ca^{2+} and Li^+ with the water molecules in their first hydration shells [26, 27]. In the case of water these predictions of a strong cation effect on the O—H stretching vibrations by the simulations have recently been confirmed experimentally for several divalent cations [28]. Strauss and Symons concluded from their IR measurements of pure methanol and of a 1,2 molal $MgCl_2$ solution at —125 °C that Mg^{2+} causes a redshift of the O—H stretching frequency of about 120 cm^{-1}. This shift is significantly smaller than that calculated here from the simulation. Considering the difficulties in attributing measured frequency shifts to single ion efects it is satisfying to see that the three site model of methanol employed in the simulation describes, at least qualitatively, the effect of the ions on the intramolecular properties of methanol. According to the relationship mentioned above, the shift of the O—H stretching frequencies caused by the ions are in good agreement with the changes in the average O—H distances of the solvation shell molecules as given in Table 4.

Acknowledgement

Financial support by Deutsche Forschungsgemeinschaft and the Hungarian Academy of Sciences is gratefully acknowledged.

1. *Marcus Y.* // Ion Solvation.— New York : Wiley, 1985.
2. *Jorgensen W. L. and Chandrasekhar J.* // J. Amer. Chem. Soc.— 1982.— **104**.— P. 4584.
3. *Impey R. W., Sprik M. and Klein M. L.*// Ibid.— 1987.— **109**.— P. 5900.
4. *Hirata F. and Levy M.*// J. Phys. Chem.— 1987.— **91**.— P. 4788.
5. *Marx D., Heinziger K., Pálinkas G. and Bako I.*// Z. Naturforsch. — 1991.— **46a**. — P. 877.
6. *Tamura Y., Spohr E., Heinzinger K., Pálinkás G. and Bakó I.*// Ber. Bunsenges. phys. Chem.— 1992.— **96**.— P. 147.
7. *Pálinkás G., Hawlicka E. and Heinzinger K.*// J. Phys. Chem.— 1987.— **91**.— P. 4334.
8. *Montague D. G. and Dore J. C.* // Mol. Phys.— 1986.— **57**.— P. 1035.
9. *Hawlicka E.*// Naturforsch Z.— 1986.— **41a**.— P. 939.
10. *Hawlicka E.*// Ber. Bunsenges. Phys. Chem.— 1984.— **88**.— P. 1002.
11. *Strauss I. M. and Symons M. C. R.*// J. Chem. Soc. Faraday Trans. Part 1.— 1977.— **73**.— P. 1796.
12. *Carney G. D., Curtiss L. A. and Langhoff S. R.*// J. Mol. Spectrosc.— 1976.— **61**.- P. 371.
13. *Bopp P., Jancsó G. and Heinzinger K.*// Chem. Phys. Lett.— 1983.— **98**.— P. 129.
14. *Jorgensen W. L.*// J. Amer. Chem. Soc.— 1981.— **103**.— P. 341.

15. *Dietz W., Riede W. O. and Heinzinger K.*// Z. Naturforsch.— 1982.— **37a**.— P. 1038.
16. *Janscó, Heinzinger K. and Bopp P.*// Ibid. — 1985.— **40a**.— P. 1985.
17. *Robinson H. L. and Symons M. C. R.*// J. Chem. Soc. Faraday Trans. Part 1.— 1985.— **81**.— P. 2131.
18. *Tanaka K., Ogita N., Tamura Y. et al.*// Z. Naturforsch.— 1977.— **42a**.— P. 29.
19. *Hawlicka E., Pálinkás G. and Heinzinger K.*// Chem. Phys. Lett.— 1989.— **153**.— P. 255.
20. *Spohr E., Pálinkás G., Heinzinger K. et al.* // J. Phys. Chem.— 1988.— **92**.— P. 6754.
21. *Szász Gy I. and Heinzinger K.*// Ibid.— 1983.— **79**.— P. 3467.
22. *Pratt K. C. and Wakeham W. A.*// J. Chem. Soc. Faraday Trans. Part 2.— 1977.— **73**.— P. 997.
23. *Heinzinger K.*// Physica.— 1985.— **131B**.— P. 196.
24. *LaPlaca S. I., Hamilton W. C., Kamb B. and Prakash A.* // J. Chem. Phys.— 1983.— **58**.— P. 567.
25. *Yamauchi S. and Kanno H.*// Chem. Phys. Lett.— 1989.— **154**.— P. 248.
26. *Probst M. M., Bopp P., Heinzinger K. and Rode B. M.*// Ibid. — 1984.— **106**.— P. 317.
27. *Tamura Y., Tanaka K., Spohr E. and Heinzinger K.* // Z. Naturforsch.— 1988.— **43a**.— P. 1103.
28. *Kleeberg H., Heinje G. and Luck W. A. P.*// J. Phys. Chem.— 1986.— **90**.— P. 4427.

Max-Planck-Institut für Chemie
(Otto-Hahn-Institut),
D-6500 Mainz, Germany
Central Research Institute for Chemistry,
Hungarian Academy of Sciences,
H-1025 Budapest, Hungary

Received 15.12.92

UDK 532/533; 536; 538.9

W. MEIER P. A. BOPP

A MODELLING STUDY OF THE CONFORMATIONAL MOTIONS OF TETRAMYDROFURANE IN VARIOUS ENVIRONMENTS

Model potentials for tetrahydrofurane (THE), including inter- and intramolecular contributions and suitable for Molecular Dynamics (MD) computer simulation studies, are constructed from literature data. In one instance the CH_2-groups are treated in the united atom approximation (one force center per group) while a second model includes all intramolecular degrees of freedom. The intramolecular motions are studied mainly by MD simulations of isolated THF molecules, THF molecules entrapped in clathrate hydrates, and of aqueous solutions of THF.

1. Introduction

Molecular Dynamics (MD) computer simulations are a very powerful tool for the study of condensed phases. Accurate and reliable microscopic interaction potentials are an essential prerequisite for such studies. For small molecules it is sometimes possible to neglect the intramolecular motions and the deformations of the molecular geometry due to the environment of the molecule. For larger molecules, however, these features can no longer be ignored nor neglected. They may even play a crucial role for the structural and dynamical properties of the condensed phase [1, 2].

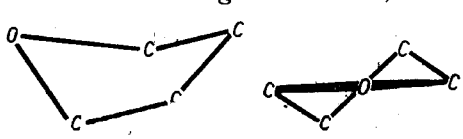

Fig. 1. The two basis conformations of THF

The properties of cyclic molecules in liquids and solids provide, among others, a good example for the importance of molecular flexibility. Tetrahydrofurane is such a molecule; many conformations of the ring are either directly. thermally accessible, or small perturbations of the intramolecular potential due to intermolecular interactions in the solid or liquid may render them accessible. There is spectroscopic evidence [3] that the equilibrium geometry of THF is nonplanar. Two such geometries can be distingushed for the THF ring: the envelope (E) form and the twisted (T) form. They are sketched in Fig. 1.